

Causal variables from reinforcement learning using generalized Bellman equations

Tue Herlau

October 30, 2020

Abstract

Many open problems in machine learning are intrinsically related to causality, however, the use of causal analysis in machine learning is still in its early stage. Within a general reinforcement learning setting, we consider the problem of building a general reinforcement learning agent which uses experience to construct a causal graph of the environment, and use this graph to inform its policy.

Our approach has three characteristics: First, we learn a simple, coarse-grained causal graph, in which the variables reflect states at many time instances, and the interventions happen at the level of policies, rather than individual actions. Secondly, we use mediation analysis to obtain an optimization target. By minimizing this target, we define the causal variables. Thirdly, our approach relies on estimating conditional expectations rather than the familiar expected return from reinforcement learning, and we therefore apply a generalization of Bellman’s equations.

We show the method can learn a plausible causal graph in a grid-world environment, and the agent obtains an improvement in performance when using the causally informed policy. To our knowledge, this is the first attempt to apply causal analysis in a reinforcement learning setting without strict restrictions on the number of states. We have observed that mediation analysis provides a promising avenue for transforming the problem of causal acquisition into one of cost-function minimization, but importantly one which involves estimating conditional expectations. This is a new challenge, and we think that causal reinforcement learning will involve development methods suited for online estimation of such conditional expectations. Finally, a benefit of our approach is the use of very simple causal models, which are arguably a more natural model of human causal understanding.

1 Introduction

A multitude of challenges for the machine learning community involve causal concepts. For instance, robustness to distributional shift between training and testing data, robustness to (minor) changes in input data as well as adversarial attacks, learning from small samples, or the learning of disentangled representations [15]. It is argued that entire classes of questions, such as counter-factual questions or simply the effect of interventions [12], can only be analyzed and answered using causal analysis. In addition to this, authors have emphasized that causation has something fundamental to do with *thinking* (i.e., reasoning about discrete concepts in an imagined space) [15].

Combining causal analysis and machine learning involves considerable bridge building. Causal analysis uses symbolic terminology such as variables and graphs, and by using structural and distributional assumptions about the data-generating mechanism in conjunction with rules a practitioner can answer various question such as an *effect size*. In contrast, machine learning has had the most success with *non-symbolic* representations, and the emphasis has traditionally been on discovering a black-box learner within some domain which simply learns by minimizing a suitable cost. Work on combining causal learning with machine learning has to negotiate these differences, and broadly speaking falls within two categories.

The first category draws on the toolkit from causal analysis and uses it to enrich machine learning. An important example is transportability, which deals with when findings of causal effects in one population can be generalized (transporter) to a new study [14], which is closely related to semi-supervised learning [4, 8]; Causal analysis has also proven useful in non-standard settings, for instance by treating latent variables in a latent-variable model of images analogous to independent causes, these have shown themselves to produce superior representations [2].

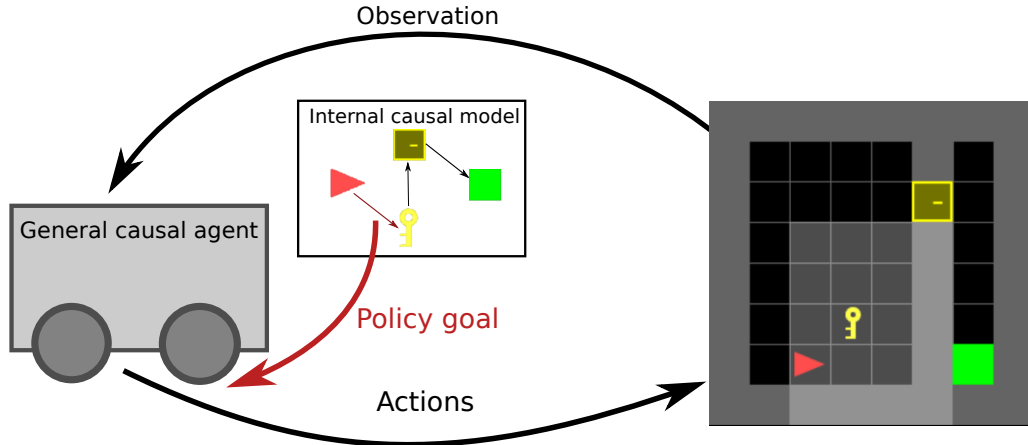


Figure 1: In the DOORKEY environment the agent (red) must learn to pick up a key to open the door and get to the goal. A general causal agent learns a small, coarse-grained causal network for the problem, and uses the causal model when training its policy.

The second category treats the problem of learning some or all parts of a causal model from data. For instance, if the noise is assumed to be additive, the causal orientation of two dependent variables can often be identified better than chance [10] and machine-learning techniques such as kernels have proven useful to overcome specific distributional assumptions [7]. A more ambitious goal is combine tests of independence, and possible directionality, to uncover aspects of the underlying causal graph of a set of observed variables [16]. Progress in this area has been severely hindered by the difficulty of reliably carrying out multi-dimensional independence tests on limited data.

This work tackles a third problem. We consider a prototypical reinforcement learning setup where the goal is to maximize the expected return, and consider how to equip a learning agent in this setup with a causal toolkit, so that it can learn a (rudimentary) causal representation of the environment suitable for obtaining a high reward. Such an agent will be referred to as a *general causal learner* (GCL) in the following.

This problem is most closely related to the problem of learning causal graphs, however it differs in that since we don't assume the observed variables are pre-defined, there will be multiple answers of what the causal graph is. To ensure the causal graph reflects relevant knowledge, the goal of the agent remains to build a reinforcement learning agent that maximize reward. In other words, our approach sees the causal graph as a means to organize knowledge and define the policy.

What we consider to be the key distinction from our approach and other more traditional causal learning setups is we will emphasize simple and crude causal graphs. This choice is partly practical, since determining a larger network of continuous variables invariantly leads to the same problems which has hindered ordinary causal graph-discovery methods. However, it has some benefits. Firstly, that if causal analysis is relevant in reinforcement learning, it is reasonable to assume a method which learns a bare minimum of causal knowledge will still see some improvement, and therefore this constitute a reasonable starting point and secondly, it makes sense to first examine ways of augment learners with the most basic and easily-interpretable causal graphs, to ensure they actually learn salient properties of the real world.

The use of very coarse graph sets the GCL apart from model-based learning, since the graph is not a model in the sense of being able to predict between adjacent time steps. It also implies the causal graph does not appear possible to fit using a generative modeling framework, since it is not a suitable model of experience, or maximum likelihood.

1.1 Example: The Doorkey environment

As an example of the problem setup, consider the DOORKEY environment (concretely, this is a modification of the gym minigrid environment[3]) in fig. 1. The agent has to pick up the key in order to open the door and get to the goal, and the environment is randomized before each episode. A single reward of +1 is given at the end of the episode upon successful termination. The agent has to apply special pickup/open actions to manipulate the key and door which makes the environment challenging for a random policy.

1.2 Observables and the binding problem

A causal graph is an equivalence class of structural models, wherein the vertices corresponds to certain variables computable from the environment (a treatment which is applied, a possible outcome, a confounder such as a patients history, and so on). We make the usual distinction between variables that are observed (observables), those that can also be manipulated (treatments), and confounding variables.

Assuming the model can be fully described as a MDP, the MDP is the true and unconfounded causal graph of the system, as it is in a matter of fact how Nature assigns a value to each observed variable. This lends to the view causal analysis should involve fairly complex, generative models of the data, which carefully takes the temporal nature of the problem into account.

However, most text-book examples of causal analysis is a great deal simpler, and only involves a few variables that have been collected prior to the analysis. A typical example is SMOKING, CANCER, and so on. Traditional causal variables therefore discards the complicated ways they are in fact generated, and corresponds to an extremely coarse aggregation of states from the real world, and retains a bare minimum of temporal ordering. This is not commonly seen as a bug, but a feature: It is exactly due to their extremely condensed form the subsequent analysis is possible, and why the results encapsulates a useful organization of knowledge (SMOKING \rightarrow CANCER). Our choice of relying on very simple, causal variables of the same form one could imagine noting in an observational study is therefore both born of a practical consideration, but also reflects our belief that trying to include the full, complicated nature of the data-generating process in the causal diagrams would be akin to loosing the baby in the bathwater.

Practically speaking, in the DOORKEY example, the candidate causal variables we have in mind would be whether the door has been opened or not, D , whether the key has been picked up or not, K , and whether the environment has been solved Y . A candidate causal graph could then be $K \rightarrow D \rightarrow Y$, but also $D \rightarrow Y$ and $K \rightarrow Y$ could be candidate graphs, and hence the problem is ill-posed. The problem of determining which states correspond to a given causal value is denoted the *binding problem* in the following, and formally consists of assigning states to configurations of causal variables.

We propose that the binding problem should be solved by a combination of two ideas. Firstly, that we define the cost function which is maximized to be a measure of causal influence, the natural indirect effect (NIE), known from mediation analysis. This measure takes the role of the expected return in a reinforcement learning setting, and therefore reduces the binding problem to a maximization problem of a certain cost function. Secondly, the terms in the cost function can be estimated using suitable generalizations of Bellman expectation equations, which allows for a theoretically well-grounded off-policy learning procedure inspired by the n -step return familiar from IMPALA [6].

Whether optimizing the cost measure will *in fact* result in a relevant causal graph will in parts be treated as an empirical question. Obviously, a successful optimization will result in a graph with a high value of the NIE, however whether this in fact solves the binding problem in a relevant way will involve examining the resulting variables. Our choice of the simple DOORKEY environment reflects it is an environment which is quite easy to study post-hoc.

1.3 Relationship to earlier work

The problem of determining causal variables has been addressed from a latent-variable perspective in image data [2, 9] as well as time-series signals using (temporal) state aggregation [19] and while especially the latent-variable representations may be of interest for further work, the inferred representations are much more complicated than the binary variables considered herein. Alternatively, the problem of determining good causal variables has been discussed extensively from a fairness-perspective, see [17] (and references therein), and while the work also makes use of the natural indirect effect the problem setup differs from the reinforcement learning task we consider. Regarding reinforcement learning, perhaps the most relevant work is [5], who applies meta-learning and show an agent is able to make causal statements over existing variables in a very limited problem setup, as well as [18], who considers an optimal treatment (intervention) regime problem from a reinforcement learning perspective. However, this past work considers the state of the MDP as comprised of just a handful of variables that can be observed and treated, which is a different setup than that considered herein where we also wish to identify the causal variables.

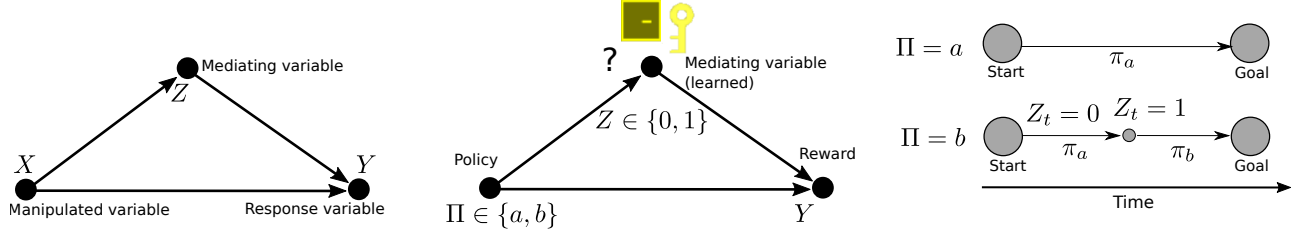


Figure 2: Left: Prototypical diagram in mediation analysis in which a cause/effect $X \rightarrow Y$ is being mediated by a variable Z . Center: Application to reinforcement learning: The manipulating variable X is considered a choice between two policies, the effect Y is the return, and Z is a (learned) variable which influence Y . We wish to quantify how the policy choice influence Y through the variable Z . Right: Choices in policy. The value $\Pi = a$ indicates we follow a baseline policy π_a . This is compared to a policy $\Pi = b$ obtained by following a policy π_b until the first time t where $Z_t = 1$ occurs, in which case we follow π_a . Both π_a, π_b and the distribution of Z_t has to be learned.

2 Methods

We consider a general reinforcement learning problem in which an agent interacts with the environment at time steps $t = 0, 1, 2, \dots$. At each time step t , the environment is in a *state* $S_t \in \mathcal{S}$, and based on the observation selects an action $A_t \in \mathcal{A}(S_t)$. One time step later, as a consequence of the agents action and the environments state, the agent obtains a numerical *reward* $R_{t+1} \in \mathcal{R} \subset \mathbb{R}$, and the environment transition to a new state S_{t+1} . The MDP and agent thereby give rise to a *trajectory*

$$(S_0, A_0), (R_1, S_1, A_1), (R_2, S_2, A_2), \dots, (R_t, S_t, A_t), \dots \quad (1)$$

The MDP is finite if the states, actions, rewards and observation all have a finite number of elements. In that case the transitions of the MDP is governed by the dynamics p which is the conditional probability action a in state s at time step t will result in a state s' and reward r in time step $t + 1$:

$$p(s', r | s, a) = \Pr(S_{t+1} = s', R_{t+1} = r | S_t = s, A_t = a). \quad (2)$$

A policy π is the probability of selecting a given action in a particular state. Specifically, if the agent follows a policy π at time step t then $\pi(a|s) = \Pr(A_t = a | S_t = s)$. We will consider an episodic setting in which the trajectory of any policy full support is of finite length with probability 1.

2.1 Mediation analysis

Mediation analysis [1, 13], in the simplest setting, is concerned with studying the effect of a treatment variable X on an outcome variable Y which is of particular interest (see fig. 2, left). For instance, X could be the application of extracurricular studies for a group of school children, and Y their academic performance at the end of the year. It is assumed the effect of X on Y may in parts be indirect, i.e. there is a third variable Z , the mediating variable, which is influenced by X and which in turn influence Y . In the example, Z could correspond to study time. Mediation analysis studies how such causal pathways can be uncovered, and how their effect can be quantified numerically.

The main quantity of interest is the *causal effect*, defined as the effect of X on Y when X is manipulated, $p(y|\text{do}(x))$, and an important goal is to determine how much of the effect of X on Y is through the direct influence $X \rightarrow Y$ and through Z , $X \rightarrow Z \rightarrow Y$.

Mediation analysis is able to quantify the extend to which a third variable such as Z mediates the effect of X on Y using various measures. Perhaps the most important measure is the *natural indirect effect* [13, 11], which measures the extend to which X influence Y but solely through Z . For a transition of $X = x$ (starting value) to $X = x'$ (manipulated value), it is defined as expected change in Y affected by holding X constant at it's natural value $X = x$, and changing Z to what value it would have attained *had* X been set to $X = x'$. This quantity involves a nested counter-factual and cannot be estimated in general, however for specific causal diagrams it

has a closed-form expression. For instance, in the simple case given in fig. 2 (left) it is defined as [11]:

$$\text{NIE}_{x \rightarrow x'}(Y) = \sum_z \mathbb{E}[Y|x, z] [P(z|x') - P(z|x)]. \quad (3)$$

The NIE has some intuitively appealing properties. It is high in the case Z is highly influenced by our choice of manipulation $X = x, x'$, meaning that Z is easy to manipulate, and the first term reflects that Z should influence the outcome Y . Meanwhile, the product implies a trade-off between these two effects. In our application let $X = \Pi$ denote our choice of policy, and then use the NIE to index good (versus bad) choices of observable variable Z and policy Π . Hence, we hypothesize that by maximizing the NIE (rather than expected return) we can address the binding problem.

2.2 Causes and effects in a reinforcement learning setting

The most natural causal variable for a causal diagram which should help the agent in its decision-making is the return

$$Y = G_0 = \sum_{t=0}^{\infty} \gamma^t R_{t+1}. \quad (4)$$

Note in the DOORKEY environment, the rewards is sparse, such that a successful completion of the environment results in a terminal reward of $R = +1$ and otherwise $R = 0$. This intuition is useful in the following, but our approach works for any reward type.

Since we consider observables as aggregates of many individual states, no single action can reasonably be considered a treatment variable. Rather, we consider a treatment equivalent to a choice of following policy a rather than b (the policies will be defined later). We denote this choice by the variable Π as

$$\Pi = a : \quad \text{Follow policy } a, \quad \Pi = b : \quad \text{Follow policy } b. \quad (5)$$

We believe this choice (rather than, say, consider the treatment variable an aggregate of states etc.) is important since it ensures a treatment is *something the agent can actually attempt to do*, rather than passively observe.

Since we are concerned with observable variables with a meaning familiar from textbook examples of causal analysis, and also since we emphasize the simplest possible case, the observables we wish to learn will be binary variables $Z = \{0, 1\}$ with the meaning that $Z = 1$ if the event Z corresponds to took place during an episode (and otherwise $Z = 0$). This definition is analogous to how SMOKING is true if the person was smoking *at some point* in the given period the study covers. Although there is just one value of Z per episode, we still need some notation to tie Z to the states of the MDP, similar to how SMOKING must correspond to certain smoking-events at given days. We therefore introduce the variables

$$Z_t \in \{0, 1\}, \quad t = 0, 1, \dots \quad (6)$$

which denotes whether Z became true at time t . As a consequence, since Z denotes if the given event took place at some point, it holds:

$$Z = \max\{Z_0, Z_1, \dots\}. \quad (7)$$

The density of Z_t , conditional on a trajectory τ , is

$$P(Z_t = z|\tau) = \text{Bern}(z \mid \theta = \Phi(s_t)). \quad (8)$$

Given these variables we can define causal graphs in the usual manner, for instance the graph

$$\Pi \rightarrow Z \rightarrow Y \quad (9)$$

would denote the case where the policy is in a causal relationship to Y by manipulating the intermediate variable Z , and the binding problem comes down to *learning* Z , by which we mean learning the function $\Phi : \mathcal{S} \rightarrow [0, 1]$.

2.2.1 Example: The Doorkey environment

Consider once more the DOORKEY environment from fig. 1. The graphs $\Pi \rightarrow Z \rightarrow Y$ or $\Pi \rightarrow Y$ would reflect either that our choice of Π affects the reward Y through Z , or that the variable Z is irrelevant and only the choice of policy matters. *What relationship is actually true depends on how we solve the binding problem*, i.e. how we choose to actually define Π and Z .

2.3 Application of mediation analysis to reinforcement learning

As the notation indicate, we let Y be the return and X , the treatment variable, be a choice of policy. The variable Z , the mediating cause, will correspond to a feature of the environment that has to be learned (see fig. 2, middle). The variable $X = \Pi \in \{a, b\}$ therefore selects between the two policies available to the agent. Inspired by the traditional relationship between X and Z in mediation analysis, we assume that if $\Pi = a$ then the agent follows a policy π_a which is trained to simply maximize Y , and otherwise if $\Pi = b$ the agent follows a policy π_b which attempts to make Z true (i.e., is trained with Z as the reward signal), and to obtain a well-defined policy, when $Z = 1$, it switches back to π_a , see fig. 2 (right). In other words, we assume the agent at time step t follows policy:

$$\pi = \begin{cases} \pi_a & \text{if } \Pi = a \\ (1 - \max\{Z_0, \dots, Z_t\}) \pi_b + \max\{Z_0, \dots, Z_t\} \pi_a & \text{if } \Pi = b. \end{cases} \quad (10)$$

Since Z and Π are binary, the NIE from eq. (3) simplifies to:

$$\text{NIE} = (\mathbb{E}[Y|Z = 1, \pi_a] - \mathbb{E}[Y|Z = 0, \pi_a]) (P(Z = 1|\pi_b) - P(Z = 1|\pi_a)). \quad (11)$$

In this notation, when we condition on π_a or π_b we mean the actions are generated from the given policy.

The NIE, with this choice, has the intuitively appealing property of being separated into a product of two simpler terms. The first involves the actual return, but also only the policy π_a . A high value of the NIE implies this difference is large, i.e. that $Z = 1$ implies a greatly increased chance of successful completion of the environment over $Z = 0$.

The second difference involves both policies but uses only Z , which is computed during a trajectory and therefore may be known long before the trajectory finishes. It implies the variable Z should be more likely to be true under policy π_b than π_a .

The trade-off excludes certain trivial definitions of Z . For instance, if $Z = Y$ the first term would be very large, however in this case π_a, π_b would be trained on the same target and so the second term should be zero.

Optimizing the target involves some technical challenges which are unfamiliar from expected-return reinforcement learning.

- The first term involves expectations conditional on Z (which depends on the trajectory). The Bellman equations (and therefore all value-function based learning) is used to estimate simple *expectation*. Obviously, for the binary case and for fixed Z this could potentially be overcome by dividing the training data into samples where $Z = 0$ and $Z = 1$, however, this solution is inelegant and does not seem to provide a valid strategy when trying to learn Z .
- The NIE is optimized both with respect to Z and π_b .

An appealing property is that when training π_b , we simply try to become better at obtaining the goal Z , which disentangles learning π_b from what may occur after the intermediate goal Z has been obtained. In other words, the proposed method naturally creates a modular policy without requiring manual specification of the intermediate goals.

In addition, the final goal Y only occurs in the left-hand parenthesis conditional on the baseline policy π_a . This suggests learning a subgoal is an off-policy task, in that the reward terms Y are all generated from the policy π_a , which could be considered fixed. It also suggests that candidate subgoals Z can be found by maximizing the left-hand parenthesis wrt. Z , i.e. classify the trajectories into those with high Y versus low Y , which is a simple classification task of trajectories generated by π_a .

We will address the problem of evaluating the NIE target in eq. (11) in two ways. Firstly, we will express the conditional terms using suitable generalizations of the Bellman expectation equations easily derived using the standard rules of probability. To take advantage of the off-policy learning method, we consider a learning method inspired by AC2, which uses V -trace estimates of the return [6].

2.4 Generalized Bellman recursions

The value function is perhaps the most important quantity in reinforcement learning:

$$v(s) = \mathbb{E}[G_t | S_t = s]. \quad (12)$$

Bellmans expectation equations $v(s_t) = \mathbb{E}[R_{t+1} + \gamma v(S_{t+1}) | S_t = s_t]$ is obtained by recursively decomposing the value function and from this the familiar methods from reinforcement learning. Comparing to the terms in eq. (11), we see the NIE involves conditional quantities. While we could attempt to simply divide the observations according to Z and train two value functions, this method would not generalize well, and furthermore it would not provide an easy way to learn Z itself. We will therefore consider a variant of Bellmans equations defined by recursively decomposing the conditional probabilities.

Suppose the length of the episode is T . For times $t \notin \{0, \dots, T\}$ we define $Z_t = 0$ for simplicity. This allows us to introduce the k variables Z_k^∞ defined as

$$Z_k^\infty = \max\{Z_k, Z_{k+1}, \dots, \} \quad (13)$$

That is, Z_k^∞ is true in the event $Z = 1$ at a time step following k . Note that

$$Z = Z_0^\infty.$$

and that the conditional probabilities obey

$$p(z_k, r_{k+1}, s_{k+1} | s_k, a_k) = p(z_k | s_k) p(r_{k+1}, s_{k+1} | s_k, a_k) \quad (14)$$

$$p(z_k | s_k) = \Phi(s_k)^{z_k} (1 - \Phi(s_k))^{1-z_k}. \quad (15)$$

We can now introduce the generalized value function:

$$V_n^\infty(s_n) = P(Z_n^\infty = 1 | s_n, Z_{n-1} = 0), \quad (16)$$

$$V_n^z(s_n) = \mathbb{E}[G_n | s_n, Z_n^\infty = z, Z_{n-1} = 0]. \quad (17)$$

Note both expressions are conditional on $Z_{n-1} = 0$. The first denotes the event Z will happen in the future starting from s_k , and the second the expected return given Z has not happened yet and either will not $z = 0$ or will $z = 1$ occur in the future. Note $V_0^z(s_0) = \mathbb{E}[G_0 | Z = z, s_0]$ and $V_0^\infty(s_0) = P(Z = 1 | s_0)$ in eq. (11). Some trivial algebra allows us to write down the decompositions (see appendix A for details):

$$V_n^\infty(s_n) = \Phi(s_n) + \bar{\Phi}(s_n) \mathbb{E}[V_{n+1}^\infty(s_{n+1}) | s_n] \quad (18a)$$

$$V_n^{z=1}(s_n) = \frac{V(s_n)\Phi(s_n)}{V_n^\infty(s_n)} + \frac{\bar{\Phi}(s_n)}{V_n^\infty(s_n)} \mathbb{E}[V_{n+1}^\infty(s_{n+1}) (R_{n+1} + \gamma V_{n+1}^{z=1}(s_{n+1})) | S_n = s_n] \quad (18b)$$

$$V_n^{z=0}(s_n) = \frac{\bar{\Phi}(s_n)}{1 - V_n^\infty(s_n)} \mathbb{E}[(1 - V_{n+1}^\infty(s_{n+1}))(R_{n+1} + \gamma V_{n+1}^{z=0}(s_{n+1})) | S_n = s_n] \quad (18c)$$

These have the same structure as the ordinary Bellman equations, but include additional terms are mutually dependent.

2.5 Off-policy learning using generalized V -trace estimators

Our overall learning approach will be to learn neural approximations of V^∞ , V and V^z as defined in eq. (18), similar to how AC2 learns a neural approximation of the value function V . This is easiest done by observing the Bellman-like recursions in eq. (18) all have the form:

$$V_n(s_n) = \mathbb{E}[S_n(s_n, s_{n+1}) + G_n(s_n, s_{n+1})V_{n+1}(s_{n+1}) | s_n] \quad (19)$$

Since we will discuss off-policy learning momentarily, we assumed all actions are generated using a *behavior policy* μ . By recursively inserting V_n in the right-hand side, we obtain the equivalent n -step return [6]:

$$V_k(s_k) = \mathbb{E} \left[\left(\sum_{i=n}^{k+n-1} \prod_{\ell=i}^{k-1} G_\ell S_k \right) + \prod_{\ell=k}^{k+n-1} G_\ell V_{k+n}(s_{k+n}) \middle| s_k \right] \quad (20)$$

Algorithm 1 General causal learner

- 1: Initialize policy networks π_a and π_b (and corresponding critic networks)
 - 2: Initialize networks $v^{z=0}$, $v^{z=1}$, v^∞ to estimate V^z and V^∞
 - 3: Initialize causal variable network Φ
 - 4: **repeat**
 - 5: Collect experience from π_a and add to replay buffer
 - 6: Sample experience from replay buffer τ
 - 7: Train π_a (and critic) using AC2
 - 8: Calculate reward signal for π_b from τ using eq. (26) and train π_b (and critic)
 - 9: Train $v^{z=0}$, $v^{z=1}$, v^∞ using n -step V -trace estimates computed using recursion defined in eq. (18) applied to experience in τ
 - 10: Train parameters in causal variable network Φ by maximizing eq. (27), where each term has been replaced by the respective V -trace estimate computed using eq. (18).
 - 11: **until** forever
-

which is a generalization of eq. (19) if $n = 1$. Suppose the current *target policy* is π , experience collected from the behavior policy μ can be used as an estimate of the return corresponding to π by using importance sampling. To reduce variance, we use a V -trace type estimator inspired by defined as [6]:

$$v_k = V(s_k) + \sum_{i=k}^{k+n-1} \left(\prod_{\ell=k}^{i-1} c_\ell G_\ell(s_\ell, s_{\ell+1}) \right) \delta_i \quad (21a)$$

$$\delta_i = \rho_i (S_i(s_i, s_{i+1}) + G_i(s_i)V(s_{i+1}) - V(s_i)) \quad (21b)$$

where c_ℓ and ρ_k are truncated importance sampling weights:

$$\rho_t = \min \left\{ \bar{\rho}, \frac{\pi(a_t|s_t)}{\mu(a_t|s_t)} \right\}, \quad c_t = \min \left\{ \bar{c}, \frac{\pi(a_t|s_t)}{\mu(a_t|s_t)} \right\} \quad (22)$$

where $\bar{\rho}$ and \bar{c} are parameters of the method. In the on-policy case where $\mu = \pi$ the V -trace estimate eq. (21a) reduces to

$$v_n = \left(\sum_{k=n}^{n+N-1} \prod_{\ell=n}^{k-1} G_\ell S_n \right) + \prod_{\ell=n}^{n+N-1} G_\ell V_{n+N}(s_{n+N}) \quad (23)$$

and is therefore a direct estimate of eq. (19); in the general case the method will provide a biased estimate when $\bar{\rho}, \bar{c} < \infty$, but the stationary policy can be analytically related to the target policy [6]. Note that the V -trace targets can be computed recursively, starting from $n + N$ and proceeding to n , as

$$v_n = V_n + \delta_n + G_n c_n (v_{n+1} - V_{n+1}) \quad (24)$$

This is the recursion which should be implemented to compute the V -trace estimates.

Remark: λ -trace estimator All of the above discussion carries through to a λ -discounted equivalent of the N -step estimator. This can be obtained by a simple change of c_n in eq. (24) to

$$v_n = V_n + \delta_n + G_n c_n (v_{n+1} - V_{n+1}), \quad c_n = \lambda \min \left(\bar{c}, \frac{\pi(a_n | s_n)}{\mu(a_n | x_n)} \right) \quad (25)$$

In which case we obtain a suitable generalization of λ -return TD learning, although one which requires complete trajectories since it is not formulated in terms of an eligibility trace.

2.6 Full method

The policy π_b in eq. (10) is trained in an episodic environment to maximize Z . Since the variable Z is multiplicative over individual time steps, we train π_b by decomposing the multiplicative cost into an equivalent sum

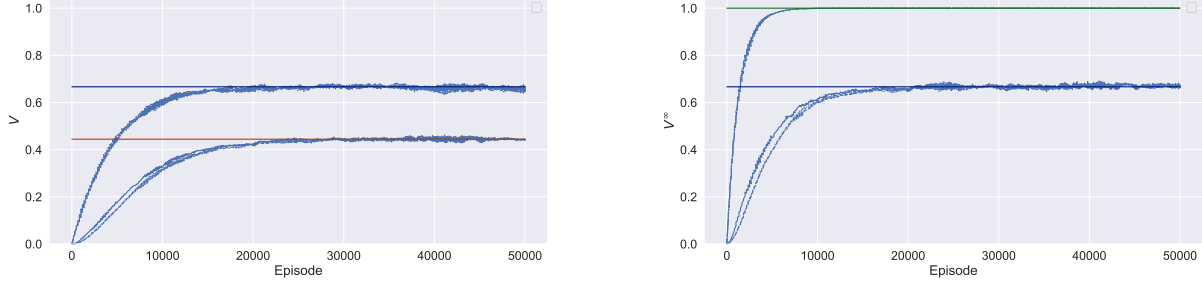


Figure 3: Trace plot of value function V and V^∞ for the TWOSTAGE environment obtained using eq. (20)

using a stick-breaking construction:

$$r_{t+1}^b = \Phi(s_t) \prod_{k=0}^{t-1} (1 - \Phi(s_k)) \quad (26)$$

which sum to $P(Z = 1|\tau)$. Hence, training on this reward signal means the policy π_b will attempt to maximize $P(Z = 1|\pi_b) - P(Z = 1|\pi_a)$ on the left-hand side of eq. (11). We can therefore train π_a and π_b using ordinary AC2 using their respective reward signals, and where the critics estimate of the return is trained against the V -trace estimate [6].

This leaves the the problem of training ϕ to maximize the NIE defined in eq. (11). Note each term can be unrolled using the V -trace estimators defined in eq. (18), thereby reducing the expression to one which expressly includes Φ , and where we can therefore train Φ by parameterizing it using a neural network and simply doing gradient descent. For instance, $\mathbb{E}[Y|Z = 1, \Pi = a]$ can be replaced by $V_0^{Z=1}$, which can be unrolled over n steps according to eq. (29a), and e.g. $\mathbb{E}[Z = 1|\Pi = a]$ can be replaced by an n -step unrolled version of V_0^∞ eq. (18a). Since the NIE is a product of two terms which are each close to zero when initialized, the actual cost function used will be of the form

$$\lambda_1 \text{NIE} + \lambda_2 (\mathbb{E}[Z = 1|\Pi = a] - \mathbb{E}[Z = 0|\Pi = a]) + \lambda_3 (\mathbb{E}[Z = 1|\Pi = b] - \mathbb{E}[Z = 1|\Pi = a]) + \lambda_4 \mathcal{H}[Z] \quad (27)$$

where in typical fashion we include an entropy term $\mathcal{H}[Z]$ to prevent trivial definitions of Z . Pseudo-code for the full procedure can be found in algorithm 1.

3 Experiments

The complete method, using value-function approximations and the NIE target in eq. (11), involves several components, and we will therefore first illustrate the generalized Bellman recursions for a simplified problem.

3.1 Example: The Twostage MRP

Since the method is based on value-function estimation, a natural testbed is a Markov Reward Process (MRP). The problem we consider is a highly idealized example of the DOORKEY environment, in which states are divided into two groups. The agent can easily transition within groups, but transitioning between groups is rarer. Between-group transition therefore acts as a bottleneck, and the group membership therefore acts as a causal variable which reflects how *far* in the environment the agent has transitioned.

Specifically, consider a finite MRP where the states are partitioned into two sets S_A and S_B as well as a goal state. The system is always initialized in a random state in S_A , and only the states in S_B has direct transitions to the goal state. To simplify the plots we choose $|S_A| = |S_B| = 3$, however this does not affect the results or long-term behavior of the system.

With probability p_{AB} the environment transition from S_A to S_B , with probability p_{AA} it transitions randomly within A and with probability p_{BB} it transitions within B . From S_B it transitions to a terminal goal state with reward 1 with probability p_{BG} , and in all cases it can transition to a terminal state (with reward zero) with probability p_D . If we use $p_{AB} = p_{BG} = \frac{2}{5}$, $p_D = \frac{1}{5}$ we obtain the $p(R = 1|s \in S_B) = p(s \in S_B|s \in S_A) = \frac{2}{3}$, $p(R = 1|s \in S_A) = \frac{4}{9}$.

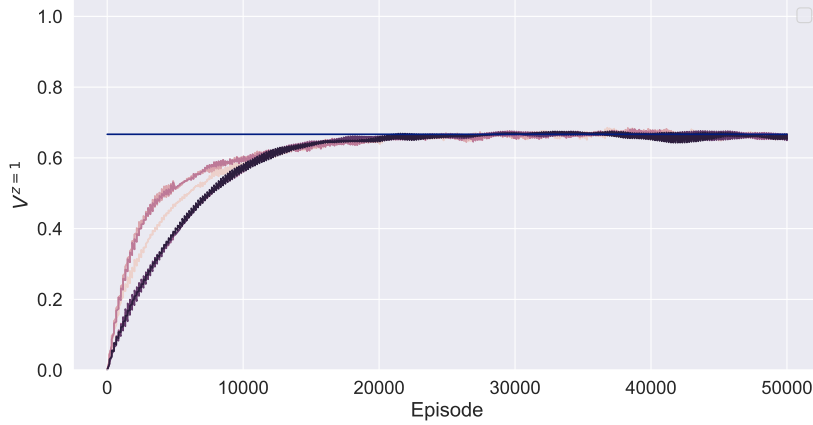


Figure 4: Trace plot of $V^{z=1}$ for the TWOSTAGE environment obtained using eq. (29c). In this case it corresponds to the probability of winning the environment given we at some point enter a state in S_B .

3.2 Tabular learning using the generalized Bellman recursions

The first example will consider how well the generalized Bellman recursions can estimate a conditional probability. In the example it is natural to let Φ correspond to whether the state is in S_B

$$\Phi(s) = 1_{S_B}(s) \quad (28)$$

The value function can be estimated using TD updates on the modified Bellman equations¹:

$$V(s_t) \stackrel{\leftarrow}{\alpha} r_{t+1} + \gamma V(s_{t+1}) \quad (29a)$$

$$V^\infty(s_t) \stackrel{\leftarrow}{\alpha} \Phi(s_t) + (1 - \Phi(s_t))V^\infty(s_{t+1}) \quad (29b)$$

$$V^{z=1}(s_t) \stackrel{\leftarrow}{\alpha} \frac{1}{V^\infty(s_t)} [V(s_t)\Phi(s_t) + (1 - \Phi(s_t))V^\infty(s_{t+1}) (r_{t+1} + \gamma V^{z=1}(s_{t+1}))] \quad (29c)$$

By iterating the simple recursions eq. (29a) and eq. (29a), the value function V and probability of membership in S_B , V^∞ , converge to their analytically expected values inserted as solid lines, see fig. 3 (further details can be found in appendix B.1).

The last recursion eq. (29c) computes $V^{z=1}$, and involves the other terms (and therefore depends on their convergence). The probability we are estimating in this case is the probability of winning given we begin in any state and *at some point* enter the states S_B ; in other words, the information we condition on is something which only occurs *at a later point* in the trajectory from the perspective of an observation $s \in S_A$, and therefore the correct estimation of this probability is not simply a matter of estimating the return for a state starting in S_B . The result is shown in fig. 4, and shows good convergence for all states to the theoretically predicted value indicated by the horizontal lines.

3.3 Learning Φ using V -trace estimation

The second example extends the TWOSTAGE environment to also learn the causal variable Φ . Since the environment has actions the terms involving π_b can be ignored in eq. (27), and we also discard the entropy term for simplicity. The objective therefore becomes:

$$\mathbb{E}[Y|Z=1] - \mathbb{E}[Y|Z=0] = \mathbb{E}[V^{z=1}(s_0) - V^{z=0}(s_0)] \quad (30)$$

The inner-most terms are rolled out using the V -trace approximation and the objective can then be directly optimized with respect to the parameters of Φ ; since this is a tabular setup, we let $\Phi(s) = \frac{1}{1+\exp(-w_s)}$, where w is the parameter vector. Further details of networks can be found in appendix B.1.

¹We use the shorthand $x \stackrel{\leftarrow}{\alpha} y$ as a shorthand for $x = x + \alpha(y - x)$

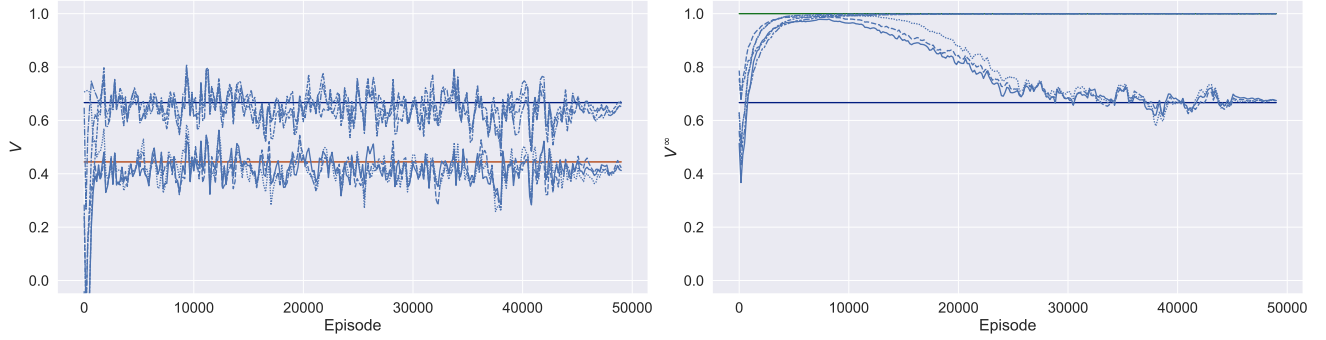


Figure 5: (Left:) Estimated value function $V(s)$ in the twostage MRP. (Right:) Probability of obtaining $P(Z = 1|s) = V^\infty(s)$ in the TWOSTAGE MRP when Φ is being learned.

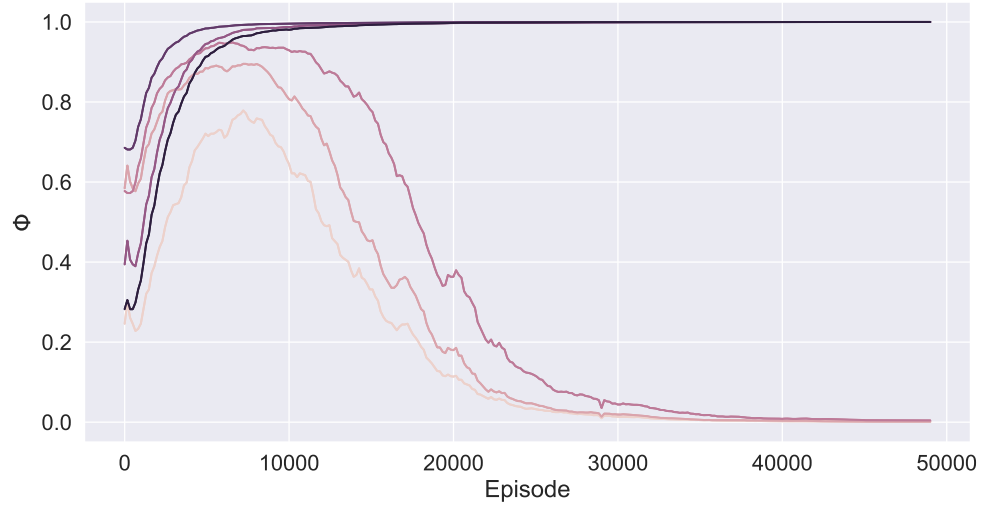


Figure 6: Value of the learned causal variable $\Phi(s)$. Colors reflect value for each of the 6 states in the TWOSTAGE MRP, and $\Phi(s)$ is the probability $P(Z_t|S_t = s)$, where Φ is learned using gradient descent.

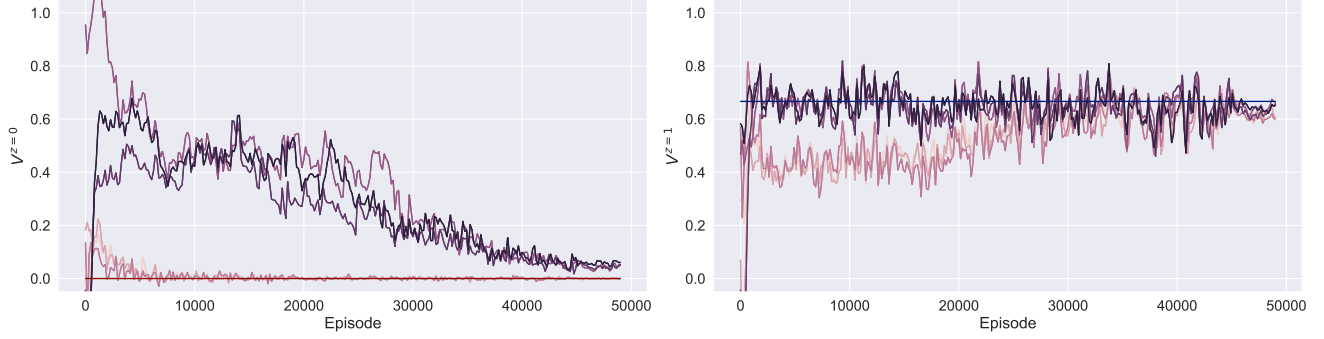


Figure 7: Probability of obtaining $P(R = 1|Z = z) = V^z$ in the TWOSTAGE MRP when Φ is being learned

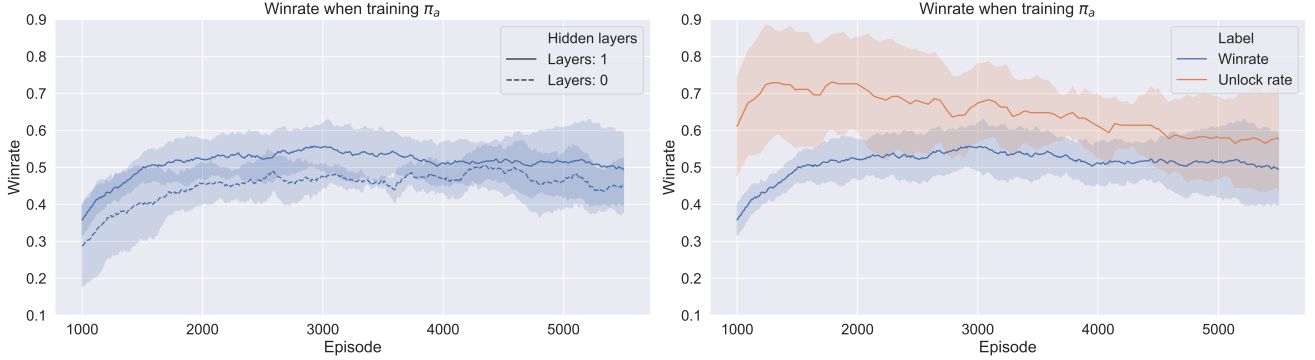


Figure 8: Accumulated reward and environment completion rate. Standard deviation reflects 8 runs and results have been smoothed over a window of 100 episodes.

The value function approximation is easily learned (see fig. 5, left) and agree with those of the TD agent (see fig. 3, left). We note the combination of a relatively high learning rate/low batch size gives rise to a fair amount of variance. The quantities V^∞ and V^z both depends on Φ , and therefore they will only begin to converge after Φ has been learned (see fig. 6). Note V^∞ is analytically simpler (see fig. 5 and converge relatively faster, meanwhile the conditional probability estimates $V^{z=1}$ involves all the other terms and converges slower (see fig. 7), but eventually converge to the analytically expected value. Note in both cases, $V^{z=1}$ should be constant for all states, and we see the method converges to this result with some fluctuation due to the constant learning rate.

3.4 Causal learning and the Doorkey environment

To apply algorithm 1 to the DOORKEY environment we first have to parameterize the states. The environment has $|\mathcal{A}| = 5$ actions, and we consider a fully-observed variant of the environment. We choose the simplest possible encoding in which each tile, depending on it's state, is one-hot encoded as an 11-dimensional vector. This means and $n \times n$ environment is encoded as an $n \times n \times 11$ -dimensional sparse tensor, and we include a single one-hot encoded feature to account for the player orientation. Further details can be found in appendix B.1.

Contrary to the TWOSTAGE environment, the method has to train two policy networks π_a and π_b using AC2 as in [6]. Since the environment encodes orientation, player position and goal position individually, and specific actions must be used when opening the door and picking up the keys, the environment is surprisingly difficult to learn and we obtain a completion rate of just about 0.5 using a 1-layer architecture after about 2000 episodes, see fig. 8 (episode length is capped to 120 in this experiment).

Since the general causal learner assumes the base policy π_a is not perfect we choose not to tune the architecture further. In fig. 8 (right) we also plot the chance of opening the door, and observe it is slightly higher than the environment completion rate. For maximizing the NIE we use the cost function eq. (27), however the parameters of the network π_b is fixed to those of π_a until half the episodes are elapsed. The method is trained for a total of $T = 50000$ episodes using a batch size of 100 (i.e., $\frac{50000}{100} = 500$ training epochs).

$\mathbb{E}[Y Z = 1]$	$\mathbb{E}[Y Z = 0]$	Δ_Y	$\mathbb{E}_{\pi_a}[Z]$	$\mathbb{E}_{\pi_b}[Z]$	NIE
0.430(20)	0.000()	0.430(20)	0.650(30)	0.870(10)	0.094(12)
0.690(60)	0.120(10)	0.570(50)	0.250(10)	0.220()	-0.018(2)

Table 1: Performance of causal agent on the DOORKEY environment and standard deviation of the mean.

	$\mathbb{E}[Y \Pi = a]$	$\mathbb{E}[Y \Pi = b]$
Causal target	0.230()	0.280()
Cross-entropy target	0.230(20)	0.270(20)

Table 2: Total reward obtain in the DOORKEY environment using baseline or causally informed policy.

To obtain a fair evaluation on separate test data, we simulate the method on 300 random instances of the DOORKEY environments, and use Monte-Carlo roll-outs of the policies π_a and π_b to estimate the quantities $\mathbb{E}[Z = 1 | \Pi = a]$, $\mathbb{E}[Z = 1 | \Pi = b]$ and so on. This therefore allows us to estimate the NIE of the graph on a separate test set.

As a means of comparison, we compare the full method in algorithm 1 against a more direct method for training the causal variable Z . The method train Φ by maximizing a cross-entropy target

$$-\mathbb{E}_{\tau} [Y(\tau) \log P(Z = z|\tau)] \quad (31)$$

rather than replaces the term $\Delta_Y = \mathbb{E}[Y|Z = 1] - \mathbb{E}[Y|Z = 0]$. In the cross-entropy target, Y is considered as a binary label and $P(Z = z|\tau)$ the (binary) regression output. In other words, we learn the variable Z as a binary classification problem of separating good (high-reward) trajectories from bad (low-reward) trajectories, where we are making explicit use of Y being binary in our particular setting, and then train π_b to maximize this target exactly as in algorithm 1. Further details can be found in appendix B.

The results of both methods can be found in table 1 (results averaged over 5 runs). The cross-entropy based learner outperforms the causal target in terms of obtaining a good separating between good versus bad trajectories, i.e. a higher value of Δ_Y . This is expected, since cross-entropy is a known, efficient cost-function for a binary classification problem.

However, the policy π_b , trained against the variable Z obtained using the cross-entropy target, does not give rise to a high NIE, which we attribute to the target being computed without consideration for how it fits with the other terms in the NIE.

To obtain insight in the causal variable we learn, we plot the causal variable $P(Z = 1)$ against both the reward, and whether the door was opened in this particular run (we add jitter for easy visualization), the result of which can be found in fig. 9. As indicated, the learned causal variable correlates well with whether the door is opened or not, and less well with the total reward. In other words, the method is able to learn that the feature of whether the agent has opened the door acts as a mediating cause in terms of completing the environment, which is a natural result considering this is a task which the agent must complete to solve the environment.

A comparable plot when training on the cross-entropy target eq. (31) is given in appendix B, however we see this causal variable does not appear to correlate well with whether the door has been opened or not.

That the causal variable corresponds to a meaningful objective is also confirmed by examining the total reward obtained from either following policy π_a , corresponding to $\Pi = a$, or the joint policy corresponding to $\Pi = b$ which can be found in table 2. Although the difference is very slight, we observe a small increase in accumulated reward for the joint policy.

4 Discussion and conclusion

The problem of combining machine learning with causal analysis, whether seen as making machine learning causally aware or using machine learning to solve tasks related to constructing causal graphs, is much easier to motivate than it is to provide such meaningful combinations, and it remains difficult to highlight specific problems machine learning currently address in which a causal approach outperforms machine learning according to a clearly defined loss or similar.

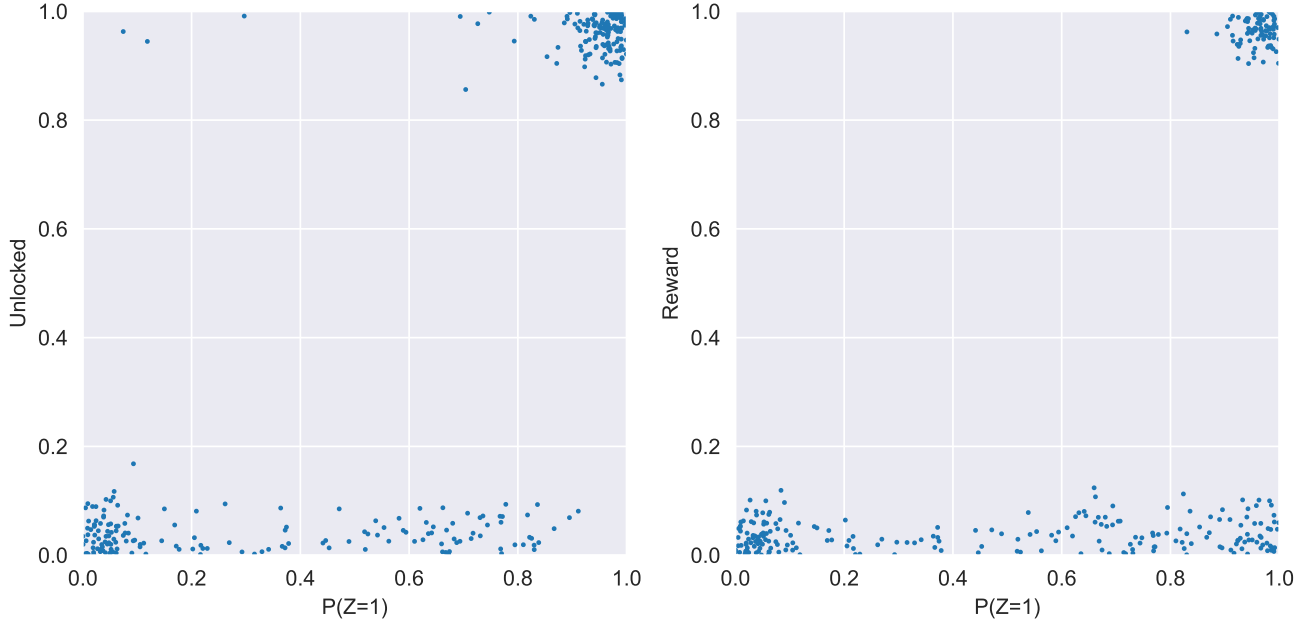


Figure 9: Scatter plot of $P(Z = 1)$ and chance of winning/unlocking door when following policy π_a

We believe the reinforcement learning setting has been under-appreciated as a testbed for causal methods, as it offers several benefits. Among these are that it is a setup in which the common interpretation of structural causal models is both true and obvious (i.e., that nodes are assigned values from temporally ordered processes), and that it allows manipulation and testing causal hypothesis.

This has the benefit that compared to e.g. the problem of learning latent representations using causal modeling, it is possible to raise the objection an application of causal analysis is a different name for latent variable learning, since the causes in these setups play similar role to latent vectors in e.g. autoencoders. We do not highlight this as a broad critique of this work, but because the problem of when a latent variable actually qualifies as a cause (and not a parameter in a machine learning model) is not clear to us at the present time.

This confusion may be partly inherent in that a causal model reflects a level of abstraction. Similar to how the classical smoking/cancer example can be described using a few binary variables, and as a complex, generative process that takes each individual into account, there cannot be an expectation that *causal reinforcement learning* means one single thing. In this regard, our work attempts to recover a very parsimonious model, which has the benefit of setting the work clearly apart from any kind of generative modeling (as well as making the conditional probabilities easy to post-hoc compute on data), however, this also comes with the drawback the causal model is not complete. For instance, we have completely ignored the problem of confounder’s, even though all quantities are obviously confounded by e.g. the maze layout. We justify this choice in two ways. Firstly, that the quantities such as the NIE are post-hoc estimated through simulations; in other words, given the definition of the variables we learn (and no other knowledge), a standard application of mediation analysis would recover our value of the NIE. Secondly, that we emphasize our application of causal analysis is not to determine the optimal causal graph, but to obtain an approximate, effective graph useful for solving the problem; as the simulations demonstrate, this is indeed what occurs, and the causal variable we recover corresponds well to an intuitive idea of causal variables as some bottleneck (both in the DOORKEY and TWOSTAGE environment) that, once we also train a policy, actually can manipulate through our actions (as in the case of the DOORKEY environment).

As to our specific approach of using generalized variants of the Bellman recursions, it is worth emphasizing other approaches are possible. For instance, one idea is to simulate trajectories from π_a and π_b directly and use these to approximate the NIE. Preliminary studies showed this method converged but was numerically quite unstable relative to the approach which uses Bellman-type recursions. The Bellman recursions can easily be generalized to non-binary variable, however we postpone this to future work. We note that combining the Bellman recursions to estimate conditional probabilities, which is a problem any application of causal analysis must address, to existing work with reinforcement learning such as [5, 18] would be of potential interest, as

would the fairly obvious generalization to Q -values rather than the value-function.

The simulations chosen in this work, namely the TWOSTAGE and DOORKEY environments, were chosen for speed and to allow easy interpretation of the causal variables, and they therefore provided a good window into the different components of the method. Although small, we emphasize the DOORKEY environment, due to the random layout and very non-linear state encoding, is non-trivial to solve using AC2. The simulations indicate the method converges, and that the causal variables obtained by maximizing the NIE is both natural within the scope of the problem, as well as gives rise to a small performance boost, indicating it is a suitable subgoal.

An obvious question to ask is how the present method can be generalized to more complex graphs of variables. Each individual pathway in the causal graph could similarly be de-composed into subgoals. If Z corresponds to e.g. opening the door, the subgoal when training on $S_0 \rightarrow Z$ could perhaps correspond to finding the key. However, constructing a full causal graph of several binary variables remains an open problem.

References

- [1] Duane F Alwin and Robert M Hauser. The decomposition of effects in path analysis. *American sociological review*, pages 37–47, 1975.
- [2] Michel Besserve, Arash Mehrjou, Rémy Sun, and Bernhard Schölkopf. Counterfactuals uncover the modular structure of deep generative models. *arXiv preprint arXiv:1812.03253*, 2018.
- [3] Maxime Chevalier-Boisvert, Lucas Willems, and Suman Pal. Minimalistic gridworld environment for openai gym. <https://github.com/maximecb/gym-minigrid>, 2018.
- [4] P Daniusis, D Janzing, J Mooij, J Zscheischler, B Steudel, K Zhang, and B Schölkopf. Inferring deterministic causal relations. In *26th Conference on Uncertainty in Artificial Intelligence (UAI 2010)*, pages 143–150. AUAI Press, 2010.
- [5] Ishita Dasgupta, Jane Wang, Silvia Chiappa, Jovana Mitrovic, Pedro Ortega, David Raposo, Edward Hughes, Peter Battaglia, Matthew Botvinick, and Zeb Kurth-Nelson. Causal reasoning from meta-reinforcement learning. *arXiv preprint arXiv:1901.08162*, 2019.
- [6] Lasse Espeholt, Hubert Soyer, Remi Munos, Karen Simonyan, Volodymyr Mnih, Tom Ward, Yotam Doron, Vlad Firoiu, Tim Harley, Iain Dunning, et al. Impala: Scalable distributed deep-rl with importance weighted actor-learner architectures. *arXiv preprint arXiv:1802.01561*, 2018.
- [7] Kenji Fukumizu, Arthur Gretton, Xiaohai Sun, and Bernhard Schölkopf. Kernel measures of conditional dependence. In *Advances in neural information processing systems*, pages 489–496, 2008.
- [8] Dominik Janzing and Bernhard Schölkopf. Semi-supervised interpolation in an anticausal learning scenario. *The Journal of Machine Learning Research*, 16(1):1923–1948, 2015.
- [9] David Lopez-Paz, Robert Nishihara, Soumith Chintala, Bernhard Scholkopf, and Léon Bottou. Discovering causal signals in images. In *Proceedings of the IEEE Conference on Computer Vision and Pattern Recognition*, pages 6979–6987, 2017.
- [10] Joris M Mooij, Jonas Peters, Dominik Janzing, Jakob Zscheischler, and Bernhard Schölkopf. Distinguishing cause from effect using observational data: methods and benchmarks. *The Journal of Machine Learning Research*, 17(1):1103–1204, 2016.
- [11] Judea Pearl. Direct and indirect effects. In *Proceedings of the Seventeenth conference on Uncertainty in artificial intelligence*, pages 411–420, 2001.
- [12] Judea Pearl. *Causality*. Cambridge university press, 2009.
- [13] Judea Pearl. *The mediation formula: A guide to the assessment of causal pathways in nonlinear models*. Wiley Online Library, 2012.
- [14] Judea Pearl and Elias Bareinboim. External validity: From do-calculus to transportability across populations. *Statistical Science*, pages 579–595, 2014.

- [15] Bernhard Schölkopf. Causality for machine learning. *arXiv preprint arXiv:1911.10500*, 2019.
- [16] Peter Spirtes, Clark N Glymour, Richard Scheines, and David Heckerman. *Causation, prediction, and search*. MIT press, 2000.
- [17] Junzhe Zhang and Elias Bareinboim. Fairness in decision-making—the causal explanation formula. In *Proceedings of the... AAAI Conference on Artificial Intelligence*, 2018.
- [18] Junzhe Zhang and Elias Bareinboim. Near-optimal reinforcement learning in dynamic treatment regimes. In *Advances in Neural Information Processing Systems*, pages 13401–13411, 2019.
- [19] Kun Zhang, Mingming Gong, and Bernhard Schölkopf. Multi-source domain adaptation: A causal view. In *AAAI*, volume 1, pages 3150–3157, 2015.

Supplementary Material

A Generalized Bellman equations

The recursive decompositions in eq. (18) can easily be proven using simple algebra. Starting with eq. (18a) and defining $\bar{\Phi} = 1 - \Phi$ and

$$\tau_k = (a_k, z_k, r_{k+1}, \dots) \quad (32)$$

a simple calculations shows that:

$$\begin{aligned} V_n^\infty(s_n) &= p(Z_n^\infty = 1 | s_n, z_{n-1} = 0) = \int dz_n p(Z_n^\infty | s_n, z_n) p(z_n | s_n) \\ &= p(Z_n^\infty | s_n, z_n = 1) \Phi(s_n) + p(Z_n^\infty | s_n, z_n = 0) \bar{\Phi}(s_n) \\ &= \Phi(s_n) + \int ds_{n+1} da_n p(Z_{n+1}^\infty | a_n, s_{n+1}, s_n, z_n = 0) p(s_{n+1}, a_n | s_n, z_n = 0) \bar{\Phi}(s_n) \\ &= \Phi(s_n) + \int ds_{n+1} da_n p(Z_{n+1}^\infty | s_{n+1}) p(s_{n+1}, a_n | s_n) \bar{\Phi}(s_n) \\ &= \Phi(s_n) + \bar{\Phi}(s_n) \mathbb{E}[V_{n+1}^\infty(s_{n+1}) | s_n] \end{aligned} \quad (33)$$

The decomposition eq. (18b) and eq. (18b) are slightly more tedious but follows from a similar argument. Focusing on the $z = 1$ case we obtain:

$$\begin{aligned} \mathbb{E}[G_n | s_n, Z_k^\infty = 1, z_{k-1} = 0] &= \int d\tau_n p(\tau_n | s_n, Z_n^\infty = 1, z_{n-1} = 0) G_n \\ &= \frac{1}{p(Z_n^\infty = 1 | s_n, z_{n-1} = 0)} \int d\tau_n p(\tau_n, Z_k^\infty = 1 | s_n, z_{n-1} = 0) G_n \\ &= \frac{1}{V_n^\infty(s_n)} \int da_n dz_n dr_{n+1} ds_{n+1} \int d\tau_{n+1} p(\tau_{n+1}, a_n, s_{n+1}, r_{n+1}, Z_n^\infty = 1 | z_n, s_n, z_{n-1} = 0) p(z_n | s_n) G_n \\ &= \frac{1}{V_n^\infty(s_n)} \int da_n dz_n dr_{n+1} ds_{n+1} \int d\tau_{n+1} p(\tau_{n+1}, Z_n^\infty = 1 | z_n, s_n, z_{n-1} = 0, a_n, s_{n+1}, r_{n+1}) p(a_n, s_{n+1}, r_{n+1} | s_n, z_n) p(z_n | s_n) G_n \\ &= \frac{1}{V_n^\infty(s_n)} \int da_n dz_n dr_{n+1} ds_{n+1} \int d\tau_{n+1} p(\tau_{n+1}, Z_n^\infty = 1 | z_n, s_{n+1}) p(a_n, s_{n+1}, r_{n+1} | s_n) p(z_n | s_n) G_n \end{aligned}$$

Which simplifies by making use of the Independence assumptions of the MDP and writing out the sum over z_n :

$$\begin{aligned} &= \frac{1}{V_n^\infty(s_n)} \int da_n dr_{n+1} ds_{n+1} \int d\tau_{n+1} p(\tau_{n+1}, Z_n^\infty = 1 | z_n = 1, s_{n+1}) p(a_n, s_{n+1}, r_{n+1} | s_n) \Phi(s_n) G_n \\ &+ \frac{1}{V_n^\infty(s_n)} \int da_n dr_{n+1} ds_{n+1} \int d\tau_{n+1} p(\tau_{n+1}, Z_n^\infty = 1 | z_n = 0, s_{n+1}) p(a_n, s_{n+1}, r_{n+1} | s_n) \bar{\Phi}(s_n) G_n \\ &= \frac{1}{V_n^\infty(s_n)} \int da_n dr_{n+1} ds_{n+1} p(a_n, s_{n+1}, r_{n+1} | s_n) \int d\tau_{n+1} [p(\tau_{n+1} | s_{n+1}) \Phi(s_n) + p(\tau_{n+1}, Z_{n+1}^\infty = 1 | s_{n+1}) \bar{\Phi}(s_n)] G_n \\ &= \frac{1}{V_n^\infty(s_n)} V(s_n) \Phi(s_n) + \frac{1}{V_n^\infty(s_n)} \bar{\Phi}(s_n) \int da_n dr_{n+1} ds_{n+1} p(a_n, s_{n+1}, r_{n+1} | s_n) \int d\tau_{n+1} p(\tau_{n+1}, Z_{n+1}^\infty = 1 | s_{n+1}) G_n \end{aligned}$$

If we focus on the right-most term we obtain:

$$\begin{aligned} &\frac{\bar{\Phi}(s_n)}{V_n^\infty(s_n)} \int da_n dr_{n+1} ds_{n+1} p(a_n, s_{n+1}, r_{n+1} | s_n) \int d\tau_{n+1} p(\tau_{n+1}, Z_{n+1}^\infty = 1 | s_{n+1}) G_n \\ &= \frac{\bar{\Phi}(s_n)}{V_n^\infty(s_n)} \int da_n dr_{n+1} ds_{n+1} p(a_n, s_{n+1}, r_{n+1} | s_n) \int d\tau_{n+1} [p(\tau_{n+1} | Z_{n+1}^\infty = 1, s_{n+1}) p(Z_{n+1}^\infty = 1 | s_{n+1})] (r_{n+1} + \gamma G_{n+1}) \\ &= \frac{\bar{\Phi}(s_n)}{V_n^\infty(s_n)} \int da_n dr_{n+1} ds_{n+1} p(a_n, s_{n+1}, r_{n+1} | s_n) V_{n+1}^\infty(s_{n+1}) \left(r_{n+1} + \gamma \int d\tau_{n+1} p(\tau_{n+1} | Z_{n+1}^\infty = 1, s_{n+1}) G_{n+1} \right) \\ &= \frac{\bar{\Phi}(s_n)}{V_n^\infty(s_n)} \int da_n dr_{n+1} ds_{n+1} p(a_n, s_{n+1}, r_{n+1} | s_n) V_{n+1}^\infty(s_{n+1}) (r_{n+1} + \gamma \mathbb{E}[G_{n+1} | Z_{n+1}^\infty = 1, s_{n+1}]) \end{aligned}$$

Parameter	Value
γ	1
α	0.001
Episodes	50000

Table 3: Simulation parameters of the tabular TD agent for the TWOSTAGE environment

The case $V_n^{z=0}$ follows from a similar argument and we obtain:

$$V_n^{z=1}(s_n) = \frac{V(s_n)\Phi(s_n)}{V_n^\infty(s_n)} + \frac{\bar{\Phi}(s_n)}{V_n^\infty(s_n)} \mathbb{E} [V_{n+1}^\infty(s_{n+1}) (R_{n+1} + \gamma V_{n+1}^{z=1}(s_{n+1})) \mid S_n = s_n] \quad (34a)$$

$$V_n^{z=0}(s_n) = \frac{\bar{\Phi}(s_n)}{1 - V_n^\infty(s_n)} \mathbb{E} [(1 - V_{n+1}^\infty(s_{n+1}))(R_{n+1} + \gamma V_{n+1}^{z=0}(s_{n+1})) \mid S_n = s_n] \quad (34b)$$

These can be compared to the standard Bellman expectation equation $V(s_t) = \mathbb{E} [R_{t+1} + \gamma v(s_{t+1})]$.

B Simulation details

B.1 Details of the Twostage simulation

The environment has a finite number of discrete states. In other words the various approximations of V , V^∞ , $V^{z=0}$ and $V^{z=1}$ all simply store a scalar number for each value. For Φ , we adopt a parameterization of the form $\Phi(s) = \sigma(w_s)$ to ensure it is within the unit interval. The long-term behavior of the TWOSTAGE environment is independent of the number of states and can be computed as:

$$p(R = 1 \mid s \in S_B) = \frac{p_{BG}}{p_{BG} + p_D} \quad (35a)$$

$$p(s \in S_B \mid s \in S_A) = \frac{p_{AB}}{p_{AB} + p_D} \quad (35b)$$

$$p(R = 1 \mid s \in S_A) = P(R = 1 \mid s \in S_B)p(s \in S_B \mid s \in S_A) \quad (35c)$$

If we use the probabilities $p_{AB} = p_{BG} = \frac{2}{5}$, $p_D = \frac{1}{5}$ we obtain

$$p(R = 1 \mid s \in S_B) = p(s \in S_B \mid s \in S_A) = \frac{2}{3}, \quad p(R = 1 \mid s \in S_A) = \frac{4}{9}.$$

B.2 Tabular Twostage experiments for fixed Φ

Details of experiment described in section 3.2. The agent simply iterates eq. (20) to convergence. In other words, for the value function the agent simply implements TD learning. The parameters used are given in table 3

B.3 Tabular Twostage experiments for learned Φ

Details of experiment described in section 3.3. The agent use algorithm 1, but simplified since there are no policies being learned. For encoding of the networks representing V , V^∞ , $V^{z=0}$, $V^{z=1}$ and Φ the agent simply stores the value of each state. All networks except Φ are trained towards their V -trace targets and Φ is trained against the cost function eq. (30). The expected results should agree with those where Φ is not learned, i.e. the learned version of Φ should be an indicator function on S_B . The on/off policy steps should be understood to mean that each time we obtain a number of episodes corresponding to the batch size the method executes a training epoch by training a given number of times on the collected batch (*on policy*) and then a number of times on data sampled from the replay buffer (*off policy*). For simplicity, this experiment uses a very small batch size and for simplicity do not use a replay buffer, which inflates the variance on the results somewhat. The parameter values can be found in table 4.

Parameter	Value
Batch size	10
On policy steps	1
Off policy steps	0
Optimizer	Adam
Learning rate	0.001
γ	0.99
Episodes	50000

Table 4: Simulation parameters of the tabular V -trace agent for the TWOSTAGE environment

Parameter	Value
Buffer size	1000
Batch size	100
On policy steps	1
Off policy steps	1
Optimizer	Adam
Learning rate	1e-05
Hidden layer size	32
λ	0.99
γ	0.99
Episodes	50000

Table 5: Simulation parameters of the V -trace agent for the DOORKEY environment

B.4 Details Doorkey simulations

We use a slightly modified variant of the **door-key** scenario from the GYM MINIGRID package [3]. The modifications are that we limit the number of actions to:

$$\mathcal{A} = \{\text{Left}, \text{Right}, \text{Forward}, \text{Pickup}, \text{Open}\}. \quad (36)$$

Note in this environment all actions are generally relevant to obtain a positive terminal reward. The reward function has been altered to be binary and only applied at the end of an episode. The environment is one-hot encoded such that each tile in the environment is an 11-dimensional vector, and a final one-hot encoding is stacked to produce a full feature vector of dimension $(5^2 + 1) \times 11$. For the simulations, we use a network with one hidden layer for the actor/critic networks for both π_a and π_b (the networks are otherwise constructed identically and trained with the same parameters). For training we use standard AC2 as described in algorithm 1. The networks approximation Φ , V , V^∞ and V^z do not contain hidden layers and are trained using standard gradient descent using the respective V -trace targets. As optimization target for Φ we use eq. (27) with $\lambda_1 = \lambda_2 = 1$, $\lambda_3 = 0$, $\lambda_4 = 0.05$, which is maximized using Adam with gradients normalized to have norm 1. We found the normalization of gradients to be important since initializations will often select extreme values in which the gradients tends to vanish. The other parameters are summarized in table 5. We note that while we use the same value of learning rates for simplicity, the gradient estimate of Φ seems to have a (relatively) higher variance than that of e.g. the policy networks, and it may be of benefit to select individual learning rates. In fig. 10 we have included a scatter plot of the learned parameter Φ when trained on the cross-entropy target, which can be compared to fig. 9.

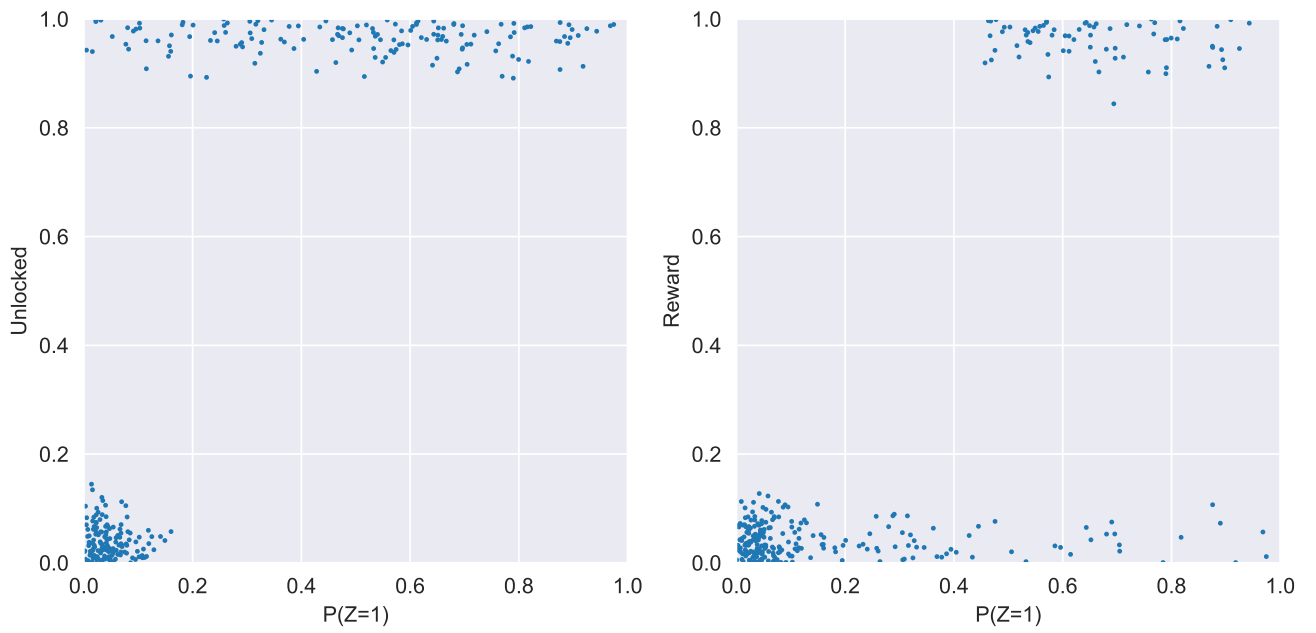


Figure 10: Scatter plot of $P(Z = 1)$ (trained on cross-entropy target eq. (31)) and chance of unlocking door or winning environment when following the policy π_a